Molecular Dynamics Study of the M_{412} Intermediate of Bacteriorhodopsin

Dong Xu, Mordechai Sheves, and Klaus Schulten
Beckman Institute and Departments of Physics and Biophysics, University of Illinois at Urbana-Champaign, Urbana, Illinois 61801

ABSTRACT Molecular dynamics simulations have been carried out to study the M_{412} intermediate of bacteriorhodopsin's (bR) photocycle. The simulations start from two simulated structures for the L_{550} intermediate of the photocycle, one involving a 13-*cis* retinal with strong torsions, the other a 13,14-*dicis* retinal, from which the M_{412} intermediate is initiated through proton transfer to Asp-85. The simulations are based on a refined structure of bR_{568} obtained through all-atom molecular dynamics simulations and placement of 16 waters inside the protein. The structures of the L_{550} intermediates were obtained through simulated photoisomerization and subsequent molecular dynamics, and simulated annealing. Our simulations reveal that the M_{412} intermediate actually comprises a series of conformations involving 1) a motion of retinal; 2) protein conformational changes; and 3) diffusion and reconfiguration of water in the space between the retinal Schiff base nitrogen and the Asp-96 side group. (1) turns the retinal Schiff base nitrogen from an early orientation toward Asp-85 to a late orientation toward Asp-96; (2) disconnects the hydrogen bond network between retinal and Asp-85 and tilts the helix F of bR, enlarging bR's cytoplasmic channel; (3) adds two water molecules to the three water molecules existing in the cytoplasmic channel at the bR_{568} stage and forms a proton conduction pathway. The conformational change (2) of the protein involves a 60° bent of the cytoplasmic side of helix F and is induced through a break of a hydrogen bond between Tyr-185 and a water-side group complex in the counterion region.

INTRODUCTION

Bacteriorhodopsin (bR) is a membrane protein that functions as a light-driven proton pump in the cell membrane of *Halobacterium halobium*. The function is achieved through a cyclic process initiated by the absorption of a photon. The pump cycle is characterized through a series of intermediates J_{625}, K_{590}, L_{550}, M_{412}, N_{520}, and O_{640}, where the subscripts denote the wavelengths of the respective absorption maxima (Lozier et al., 1975).

A major role in the proton pump cycle of bR_{568} is played by its retinal chromophore, which is bound through a Schiff base linkage to the Lys-216 residue. Retinal undergoes an initial electronic excitation and photochemical transformation. It also acts as a switch, donating a proton to the extracellular side of bR_{568} and accepting a proton from the intracellular side. Retinal and the numbering adopted for its atoms and dihedral angels are presented in Fig. 1.

In bR_{568}, retinal is in an *all-trans* configuration as shown in Fig. 1. A photon triggers an isomerization of retinal and leads to the transition $bR_{568} \rightarrow J_{625}$. The intermediate J_{625} decays thermally to K_{590} and then relaxes to L_{550}, at which point retinal is in a 13-*cis* state (Doig et al., 1991). Possible torsions of bonds other than the 13–14 bond of retinal (Fig. 1) were suggested, as discussed below. During the $L_{550} \rightarrow M_{412}$ transition, retinal's Schiff base proton is transferred to Asp-85 (Mogi et al., 1989; Braiman et al., 1988; Gerwert et al., 1989; Metz et al., 1992) to be released eventually to the extracellular space. Retinal remains in a 13-*cis* isomeric state in the M_{412} intermediate (Pettei et al., 1977; Aton et al., 1977). During the subsequent transition $M_{412} \rightarrow N_{520}$, a proton is transferred to retinal's Schiff base from Asp-96; the latter side group eventually takes up a proton from the cytoplasmic environment (Gerwert et al., 1989). The photocycle is completed as retinal returns to an *all-trans* isomeric state and the protein returns to bR_{568}, either through the O_{640} intermediate or directly from N_{520} (Váró et al., 1990).

The M_{412} intermediate serves as a switch between a proton release pathway and a protein uptake pathway (Nagle and Tristram-Nagle, 1983; Braiman et al., 1988; Papadopoulos et al., 1990; Gerwert, 1992), the switch disconnecting retinal from the extracellular side and connecting it to the cytoplasmic side (Orlandi and Schulten, 1979; Váró and Lanyi, 1990, 1991a, 1991b). The processes underlying this switch are not known, and it is fair to claim that the elucidation of these processes holds the key to the eventual discovery of the mechanism of bR.

A key difference between explanations of bR's proton pump mechanism lies in the separate roles of retinal and the protein in realizing the switch function at the M_{412} stage. According to Fodor et al. (1988), the switch is realized through a protein conformational change, with retinal remaining in the same 13-*cis* geometry in the L_{550} as well as in the M_{412} intermediate. Another model (Schulten and Tavan, 1978; Schulten, 1978; Schulten et al., 1984; Gerwert and Siebert, 1986) suggests that retinal is in a 13,14-*dicis* configuration in the K_{590} and L_{550} intermediates, and that it

Received for publication 25 May 1995 and in final form 22 August 1995.

Dr. Xu's current address: Laboratory of Mathematical Biology, NCI/Frederick Cancer Research and Development Center, P.O. Box B, Building 469, Frederick, MD 21702.

Dr. Sheves' permanent address: Department of Organic Chemistry, The Weizmann Institute of Science, Rehovot 76100, Israel.

Address correspondence to Dr. Klaus Schulten, Department of Physics, Beckman Institute-3147, University of Illinois, 405 N. Mathews Ave., Urbana, IL 61801. Tel:217-244-2212; Fax: 217-244-6078; E. Mail: kschulte@ks.uiuc.edu.

0006-3495/95/12/2745/16 $2.00

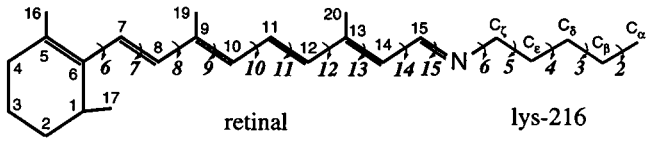

FIGURE 1 Numbering of carbon atoms and dihedral angles of retinal and the Lys-216 aliphatic chain. The numbers in Roman represent the numbering of the carbon atoms of retinal; the numbers in bold italic represent the numbering of dihedral angles.

functions as a switch through a torsional motion around the 14–15 bond in the M_{412} intermediate.

The arrangement of the retinal chromophore and of key amino acid side groups, as reported in Henderson et al. (1990), supports the notion of a proton channel controlled by retinal. Unfortunately, the low resolution structure in Henderson et al. (1990) does not reveal water, which is expected to play a crucial role in proton conduction. Protein structural transformations amounting to a widening of the cytoplasmic channel have been observed for the M_{412} intermediate (Dencher et al., 1992; Subramanian et al., 1993; Hauss et al., 1994) and should be invoked in an explanation of the switch function of this intermediate. However, the available structural information does not yield an explanation of the pump mechanism, in particular, of the switch mechanism of M_{412}.

Molecular dynamics simulations appear to be suited to provide the missing information, i.e., to place the unresolved water, initiate the phototransformation, and follow the intermediates of the pump cycle up to the M_{412} stage. But such procedures are methodologically extremely demanding, if possible at all, due to several factors: 1) the low resolution structure in Henderson et al. (1990) may contain serious, i.e., misleading, errors; 2) placement of waters by means of computer modeling is difficult; 3) reliable potential surfaces of retinal in the excited state do not exist and, hence, the phototransformation can only be described through *ad hoc* models, which induce the observed *all-trans* → 13-*cis* transformation of retinal; 4) the pump cycle up to the formation of M_{412} requires a time span of microseconds, i.e., a time period too long for conventional molecular dynamics descriptions, but possibly amenable to the simulated annealing method. The difficulties of molecular dynamics descriptions in general, e.g., the limited reliability of the force fields used, and the shortcomings (1–4) in particular, make modeling of the M_{412} intermediate necessarily a highly speculative effort. However, the previous studies of the intermediates up to the L_{550} stage (Humphrey et al., 1994; Humphrey et al., 1995), as outlined below, consistently lead to a small number of candidate structures; the two most pertinent of these structures, referred to as L_1 and L_2, will be investigated in the present study. The results imply that one of the structures, namely L_1, leads to an M_{412} intermediate that is in excellent accord with observations and extremely interesting in that the long standing dispute between the above mentioned models for the M_{412} switch function is resolved. Our study suggests that key single bond torsions of retinal, internal waters, and a protein conformational change cooperatively contribute to the switch function of the M_{412} intermediate.

Several molecular dynamics calculations were carried out to shed light on the pump mechanism of bR (Warshel et al., 1991; Bashford and Gerwert, 1992; Scharnagl et al., 1994). One of the early simulations (Zhou et al., 1993) attempted to describe the whole pump cycle by forcing proton transfer reactions to occur on a time scale covered by molecular dynamics simulations, i.e., on a time scale of 100 ps, rather than on the observed millisecond time scale. The simulations revealed that retinal at the M_{412} stage of bR, i.e., after transfer of the Schiff base proton, can act as a proton switch in that the Schiff base nitrogen turns spontaneously from an orientation toward Asp-85 (the proton acceptor) to an orientation toward Asp-96 (the proton donor) after the retinal → Asp-85 proton transfer.

Based on a refined structure of bR_{568} (Humphrey et al., 1994), simulations have been carried out to study the early intermediates J_{625}, K_{590}, and L_{550} (Humphrey et al., 1995). The simulations, sampling different initial conditions, yield a distribution of reaction products falling into four distinct classes: class I, *all-trans* retinal; class II, 13-*cis* retinal with the Schiff base proton oriented toward Asp-96; class III, 13-*cis* with the Schiff base proton oriented perpendicular to the membrane normal (see Fig. 2 (L_1)); and class IV, 13,14-*dicis* (see Fig. 2 (L_2).) To reach the microsecond time scale of formation of the L_{550} intermediate, the study in (Humphrey et al., 1995) employed simulated annealing. The simulations in Humphrey et al. (1995) identified two likely structures for the L_{550} intermediate: one, referred to as L_1 below, involves a 13-*cis* retinal with a strong torsion; the other, referred to as L_2 below, involves a pure 13,14-*dicis* retinal.

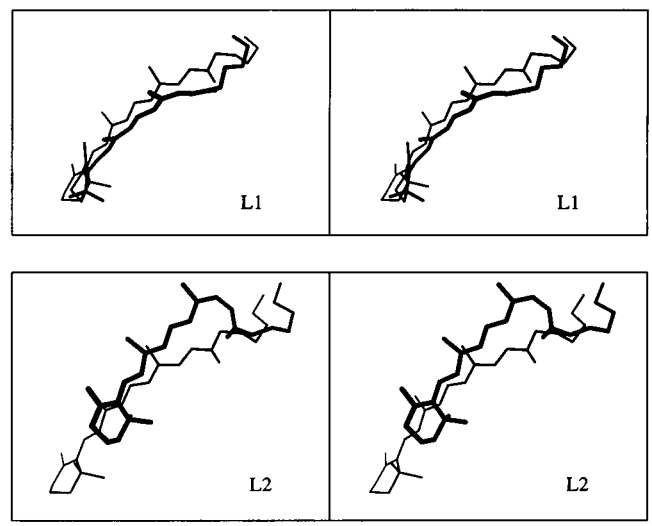

FIGURE 2 Stereoviews of retinal in the structures L_1 and L_2 (*bold*) superimposed on retinal in bR_{568} (*thin*). There is no center of mass movement or overall rotation of the whole bR from bR_{568} to L_1 or L_2.

The structure of L_1 is presented in Fig. 3. The figure shows the three regions of the proton pathway in bR: 1) the cytoplasmic channel, the space between Asp-96 and the Schiff base including the amino acid side groups Thr-46, Leu-93 and Phe-219; 2) the counterion region, the space near the retinal Schiff base and its counterions including Asp-85, Tyr-57, Tyr-185 and Asp-212; 3) the extracellular channel, the channel between the counterions of the Schiff base and the extracellular side of bR, including the regions around Arg-82, Glu-204 and Glu-9.

In the present paper we employed the L_{550} structures described in Humphrey et al. (1995) to initiate the M_{412} intermediate through transfer of the retinal proton to Asp-85. The following sections describe the methods employed, the results obtained, comparisons with observations, and the emerging explanation of the mechanism of the light-driven proton pump realized by bacteriorhodopsin.

METHODS

The simulations and analyses described in this paper were carried out using the program X-PLOR (Brünger, 1992) together with the CHARMm force field (Brooks et al., 1983). A cut-off distance of 8 Å for non-bonded interactions and a dielectric constant $\varepsilon = 1$ were employed. An integration timestep of 1 fs was chosen. Like the simulations of bR_{568} reported in Humphrey et al. (1994), and of the J_{625}, K_{590}, L_{550} intermediates reported in Humphrey et al. (1995), we employed an all atom model and an explicit hydrogen bonding term in the energy function, both of which are particularly important for the placement of water inside bR.

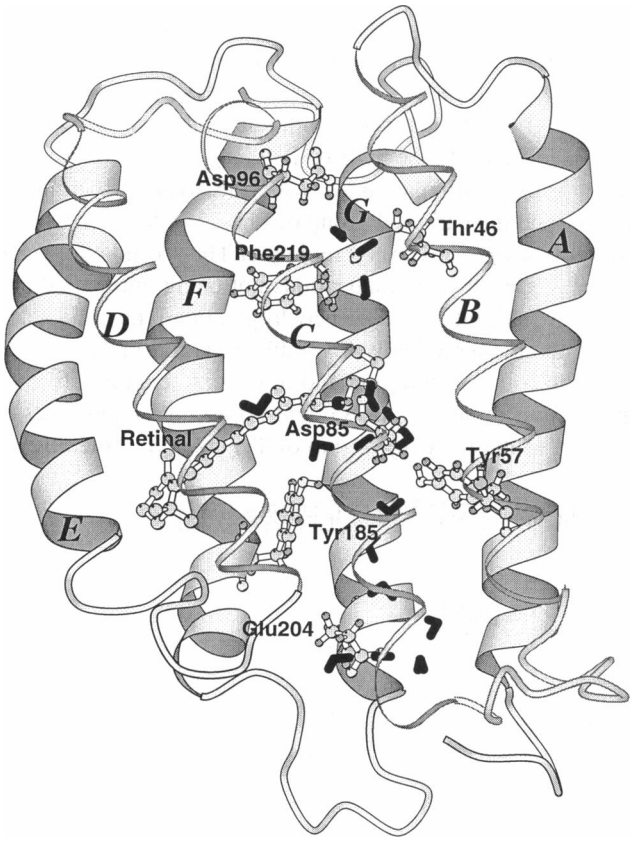

FIGURE 3 Ribbon diagram of L_1, showing retinal, key amino acid side groups, and water molecules (the latter in *solid black*). This figure and Figs. 9 and 15 were generated with MOLSCRIPT (Kraulis, 1991).

Following Humphrey et al. (1994) and Humphrey et al. (1995), the protonation states of titratable groups adopted were standard except for Asp-85, Asp-96, and Asp-115, which were assumed to be protonated according to observations reported in Gerwert et al. (1989) and Engelhard et al. (1990). The force field parameters and charges used for bR were, respectively, the parmallh3x.pro paramaters and topallh6x.pro charges, except for retinal. For the deprotonated and the protonated Schiff base retinal in bR, we adopted the charges suggested in Zhou et al. (1993), except for changes to fit the explicit hydrogen model, i.e., the explicit hydrogen atoms added to the retinal backbone were given partial charges of 0.03, with the corresponding heavy atom charges reduced by the same amount. The force field parameters for the protonated Schiff base retinal were those used in Humphrey et al. (1994) (1995). The unprotonated Schiff base retinal is assumed to have the same force field parameters as those of the protonated one except that the 13–14, 14–15 and 15-N torsion force constants were 30, 5, and 30 Kcal/mol, respectively, as suggested in Zhou et al. (1993).

Water was placed in the interior of the protein to simulate photocycles in early studies (Warshel et al., 1991; Zhou et al., 1993; Humphrey et al., 1994; Scharnagl et al., 1994). In the present study, 16 water molecules were placed inside bR in the structures of L_{550} (see Fig. 3) (Humphrey et al., 1995). Seven water molecules were placed in the counterion region, three in the cytoplasmic channel, and six in the extracellular channel. These water molecules were described by a TIP3P potential (Jorgensen et al., 1983) with the CHARMm parameter file param19.sol. The 16 water molecules, however, do not include all the possible waters in bR; in placing these waters we focused on the retinal binding site, on the cytoplasmic channel, and on the extracellular channel where we filled all voids that were sufficiently hydrophilic as judged, e.g., by the stability of the water positions. Voids in other parts of bR were disregarded for water placement because we considered respective waters to be less relevant to the photocycle (Zhou et al., 1993; Humphrey et al., 1994).

Simulated annealing

The times for the formation and decay of the M_{412} intermediate are in the μs and ms range; presently, computational resources allow one to cover time periods of only a few nanoseconds in molecular dynamics simulations. For a description of the M_{412} intermediate we resorted, therefore, to simulated annealing (van Laarhoven and Aarts, 1987; Brünger et al., 1990; Brünger, 1991).

Annealing involves coupling of the simulated system to a heat bath that is kept at a prescribed temperature and is modulated during the simulation. The bath temperature follows a certain schedule of heating and cooling. Temperatures $T \geq 600$ K adversely affected the structure of bR. Wishing to employ the highest possible temperatures to accelerate the reaction dynamics of our system, we accepted 500 K as the highest annealing temperature because this temperature left the overall structure of bR intact for sufficiently long times, but produced rapid local conformational changes.

For the conventional choice of a barrier of 5 kcal/mol for torsion around the single bonds of retinal, particularly around its 8–9 and 10–11 bonds, the high temperatures chosen in the annealing schedule render the chromophore too flexible. To prevent unrealistic torsions, we constrained all single bond dihedral angles along retinal's backbone by raising their barriers to 10 kcal/mol during the simulated annealing steps. The SHAKE algorithm for constraining bond lengths was used for all temperatures elevated above 300 K to keep the numerical integration stable for a 1-fs time step. The high torsional barriers and the SHAKE constraints were released during the 300 K equilibration phases of the simulations.

Replacement of water

During the photocycle, the conformation of bR changes. We suggest that this change allows water molecules to diffuse into the cytoplasmic channel

of bR. To mimic the process of additional waters entering the cytoplasmic channel, we removed water molecules from the exit of the extracellular channel and moved the channel to the desired position. Since most structural transitions at the M_{412} stage occur in the cytoplasmic channel and in the counterion region, the removal of water from the far extracellular region is unlikely to affect the dynamics at the M_{412} stage.

Summary of simulations

As explained above, our simulations started from two structures suggested in Humphrey et al. (1995) for the of L_{550} intermediate, L_1, and L_2. Our simulations transferred a proton from the retinal Schiff base to Asp-85 and carried out energy minimization, molecular dynamics simulations, and annealings. The structures obtained from L_1 and L_2 after proton transfer and equilibration will be referred to as M_a and MI_a, respectively. Structures obtained after further simulations will be similarly denoted as M_b, M_c, etc. and MI_b, MI_c, etc. The simulations to generate later stages of the respective M_{412} intermediates are summarized and defined in Fig. 4.

RESULTS

As mentioned above, in our simulations we have investigated two models for the M_{412} intermediate, one starting from the L_1 candidate structure for the L_{550} intermediate shown in Fig. 3 and one starting from the L_2 structure. During the M_{412} stage in both models, bR undergoes a series of transformations induced by simulated annealing and equilibration steps summarized in Fig. 4. The induced transformations include structural rearrangements of retinal, alterations in the helices of bR as well as a rearrangement of waters and their hydrogen bond network.

Simulation of an M_{412} intermediate starting from L_1

We will consider first the evolution of bR in the case that the M_{412} stage is initiated through a retinal → Asp-85 proton transfer of L_1 (see Fig. 3 and the subsequent simulations summarized in Fig. 4(a)).

The M_a state

The state of bR, obtained following the Schiff base proton transfer of L_1 to Asp-85 and subsequent equilibration, is referred to as the M_a state. Fig. 5 compares the geometry of retinal in this state with the retinal geometry in bR_{568}. For M_a the retinal backbone from C_6 to C_{13} (the numbering of retinal's carbons is defined in Fig. 1) is tilted significantly, and the C_{20} methyl group is shifted by 1.68 Å toward the cytoplasmic side relative to its position in bR_{568}. The retinal structure is in agreement with the report by Hauss et al. (1994), which shows that in M_{412} the polyene chain tilts out of the plane of the membrane toward the cytoplasm by $\sim 11° \pm 6°$. The 1.68 Å shift is also in agreement with observations reported by Heyn and Otto (1992), which showed that the $bR_{568} \rightarrow M_{412}$ transformation tilts the transition dipole moment of retinal out of the plane of the membrane and moves the C_{20} methyl group by 1.7 Å toward the cytoplasmic side of the membrane.

Fig. 6 presents the dihedral angles of retinal in the M_a state. Significant deviations of the angles from the equilibrium values exist, e.g., the dihedral angle of the 14–15 bond assumes a value of 201.4°. Functionally, the most significant feature of the retinal structure at the M_a stage is the orientation of the Schiff base and its two neighboring carbon atoms in a direction nearly parallel to the membrane plane. Such conformation of retinal is accommodated by a strained Lys-216 side chain, the dihedral angles of which are shown in Fig. 7.

The configuration of waters, amino acid side groups, and hydrogen bonds of M^a is presented in Fig. 8. The figure shows three water molecules (A, B, and C), which were placed in the cytoplasmic channel as reported by Humphrey et al. (1994). At the M_a stage, two of the three waters (A and B) strongly hydrogen-bond with each other. Water A also hydrogen-bonds to the hydroxyl moiety of Asp-96. Water B also forms hydrogen bonds with the hydroxyl group of Thr-46 and the carbonyl group of Phe-219. Water C weakly connects with the hydroxyl moiety of Thr-46 and with water B, the angles of both connections not being optimal. Water C did not exhibit any further hydrogen bond, i.e., this water is not in an energetically favorable situation in M_a.

In the counterion region and in the extracellular channel, three water molecules (F, G, and H) arrange themselves to connect to the hydroxyl group of Tyr-57 and to the oxygen

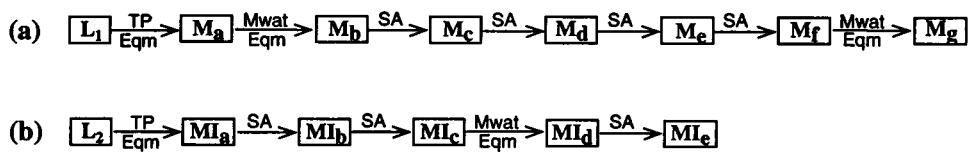

FIGURE 4 Calculations carried out for the L_1 pathway (*a*), and for the L_2 pathway (*b*). The notations used in the figure are: TP, transfer of a proton from the retinal Schiff base to Asp-85, followed by 200 steps of conjugate gradient minimization; Eqm, 20-ps molecular dynamics equilibration at $T = 300$ K, followed by a 200-step minimization; Mwat - movement of a water molecule to a position into the cytoplasmic channel, again followed by a 200-step minimization; SA, simulated annealing employing the soft constraints for the single bond dihedrals along retinal's backbone carrying out the following steps: 1) 100-step minimization; 2) starting at 500 K: 100 fs simulation, use of *T*-coupling (Brünger, 1992) to rescale velocities with a friction constant of 100 ps^{-1}; then a 50-step minimization and reassignment of velocities corresponding to 490 K; again a 100-fs simulation and a 50-step minimization; same procedures at 480 K, 470 K, and so on, until 300 K was reached (the frequent reassignment of velocities facilitates the search for a wider conformational space, and the 50-step minimization before reassignment of velocities helps to avoid instabilities due to velocity redistributions); 3) the process in (2) above was repeated, but starting from 400 K. After procedures 1–3 were completed, soft constraints for the single bond torsions along retinal's backbone were released and a 10-ps molecular dynamics equilibration at $T = 300$ K was carried out; a 200-step minimization completed the simulated annealing.

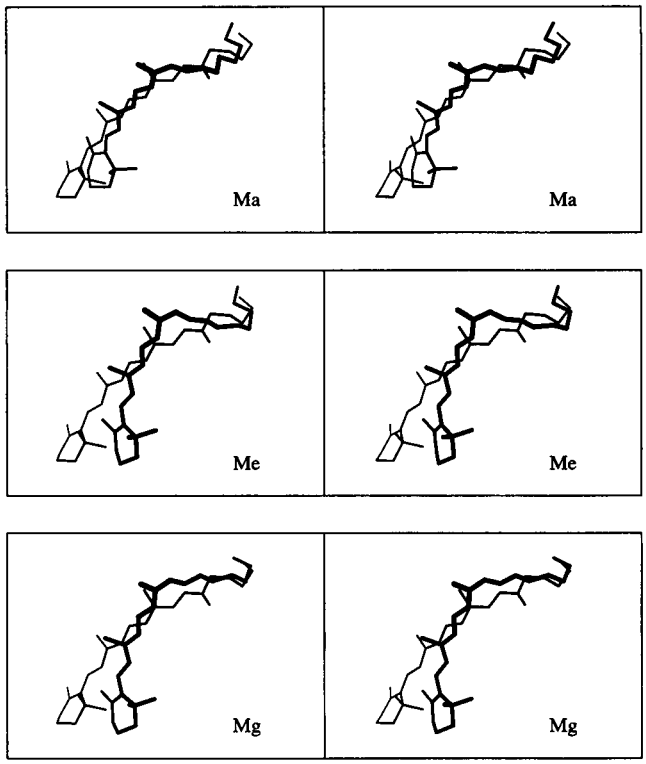

FIGURE 5 Stereoviews of retinal at the M_a, M_e, and M_g stages (*thick*) superimposed on retinal in bR_{568} (*thin*). There is no center of mass movement or overall rotation of the whole bR from bR_{568} to M_a, M_e, or M_g.

group of the Thr-89 hydroxyl moiety (Fig. 8). Water G connects to water I, which hydrogen-bonds to an oxygen of the Asp-212 carboxylate. Water F, which connects to Thr-89, develops a strong hydrogen bond to the Schiff base. Water H hydrogen-bonds to Tyr-57 as well as to the carboxylate oxygen of Asp-212. Waters F, G, and H develop a strong hydrogen bond among each other; the hydroxyl groups of these waters lie approximately on a line, and the planes of these waters are nearly coplanar. The hydroxyl group of Asp-85 lies almost perpendicular to this water plane. The distance between the hydrogen of the hydroxyl group in Asp-85 and its closest possible hydrogen bond acceptor, the oxygen of water G, is 2.44 Å. Neither oxygen of the Asp-85 carboxylate has a close donor to form a good hydrogen bond and, as a result, Asp-85 is not interacting with the water chain F, G, and H.

The total root mean square deviation (RMSD) between the structure of M_a and that of L_1 measures 2.51 Å, which is actually larger than the RMSD values experienced during later stages of M_{412}. In fact, in going from L_1 to M_a significant overall protein conformational changes develop, in particular, a large bend of helix F of ~60° away from the center of bR. This bend is localized around Arg-175, Asn-176, and Val-177 as shown in Figs. 9 and 10. Within 1 ps after the retinal → Asp-85 proton transfer from L_1, i.e., during the equilibration (at 300 K) period, the hydrogen bond between the NH of Val-179 and the backbone carbonyl oxygen of Arg-175 (a typical hydrogen bond of α-helix) broke, and these moieties separated from a distance of 2.26 Å to a distance of 4.5 Å. The carbonyl of Arg-175 developed, and then a hydrogen bond to the hydroxyl of Thr-178 and helix F started to bend. We suggest that this bend widens the cytoplasmic channel of bR.

A significant conformational change is also exhibited by the cytoplasmic portion of helix G at the M_a stage. Helix G moved by ~1Å away from the waters between Asp-96 and the retinal Schiff base toward helix F. Our simulations appear to be in agreement with observations of changes in bR's electron density at the M_{412} stage as observed in Hauss et al. (1994). In our simulations, helix E experienced a translational shift of about 2 Å toward the center of bR, but otherwise the conformation of helix E did not change as much as that of helices F and G. No significant change was observed for helices A, B, C, and D.

Concomitant with the bend of helix F, the ring of Tyr-185 on the extracellular side of this helix moved relative to bR_{568} by about 3.8 Å away from the Schiff base toward the extracellular side and toward retinal's β-ionone ring. This significant motion, shown in Fig. 10, is because of a weakening of the interaction of Tyr-185 with the hydrogen bond network of waters F, G, I, H (Fig. 8) after the retinal → Asp-85 proton transfer. As a result of the motion of Tyr-185, the extracellular side of helix F including Pro-186, moved down and away from the center of the protein by ~3 Å, whereas the hydrogen bond pattern of the helix backbone did not change significantly, i.e., no tilt developed in the portion of the helix around Tyr-185 and Pro-186. Pro-186 remains in close contact with retinal's β-ionone ring throughout the early pump cycle up to the M_{412} stage. This implies that the conformational changes around Tyr-185 and Pro-186 are induced by the ring of retinal, as well by the hydrogen bond between Tyr-185 and the water-side group complex in the counterion region. Helix F around Trp-182 moved very little because of the bulky size of tryptophan, whereas the torsion angle of C_α-N of the Trp-182 backbone varied from 70.66° in bR_{568} and 66.89° in L_1 to 97.15° in M_a. Hence, Trp-182 can be considered a hinge for the motion of the helix.

From M_b to M_f

When we applied further annealing to M_a, the waters in the counterion region and in the extracellular channel did not change their configuration, whereas the waters in the cytoplasmic channel altered their arrangement. The rearrangement arose because waters, at this stage, did not fill any more all-accessible voids in the cytoplasmic channel; and therefore the waters became too mobile to form a stabilized configuration.

The conformational change of helix F and helix G introduced cavities in the cytoplasmic channel that provide space for further water molecules (Fig. 10). Accordingly, we placed one water (water D), originally positioned on the far extracellular site in M_a, between the retinal Schiff base and

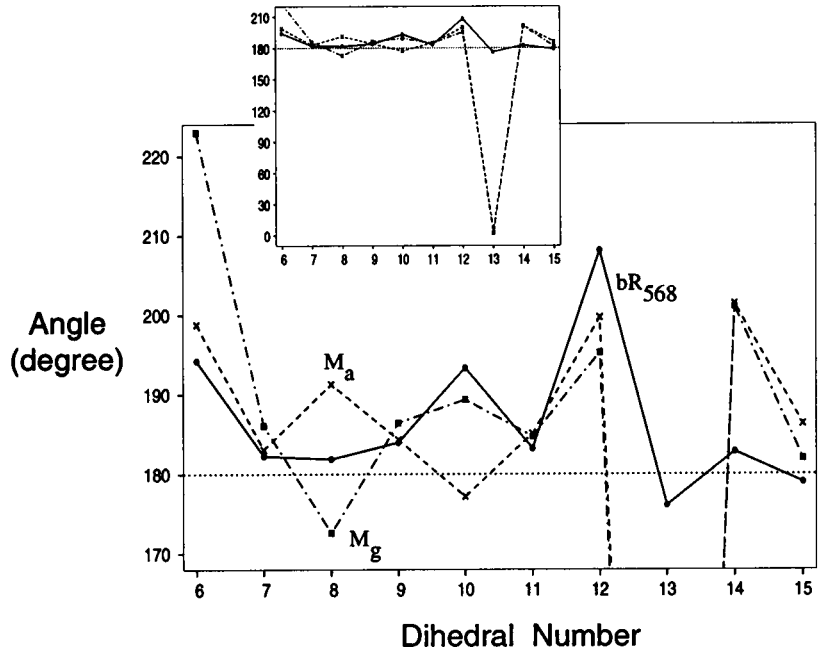

FIGURE 6 Comparison of the dihedral angles along retinal's backbone in M_a, M_g, and bR_{568}. The numbering of dihedral angles is defined in Fig. 1. The larger plot is a magnification of the smaller one.

water C. Water D did not remain in this position, but rather moved toward Asp-96 to connect with waters B and C. This placement established a connection between the hydroxyls of Asp-96 and of Thr-46 and the carbonyl of Lys-216 through waters A, B, C, and D.

In M_c, waters C and D remained at their place, but the hydrogen bond between water A and the hydroxyl of Asp-96 broke, and these waters moved toward the Schiff base. The four water molecules, A, B, C, and D, formed a hydrogen bond network.

In M_d, the four water molecules in the cytoplasmic channel kept the same arrangement as in M_c. One interesting feature is that waters B and D exchanged their position, which implies that there were still cavities in their vicinity. A small rearrangement between these four water molecules indicates a suboptimal hydrogen bond network in M_d

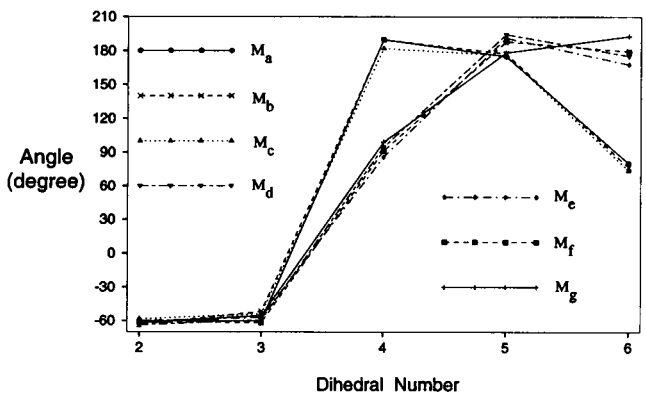

FIGURE 7 Comparison of the dihedral angles along the Lys-216 aliphatic chain for the states from M_a to M_g. The numbering of dihedral angles is defined in Fig. 1.

that may drive the subsequent dynamics of the M_{412} intermediate.

At the M_e stage, the hydrogen bonds between waters A, B, C, and D became even more unstable, the water closest to the retinal Schiff base, i.e., water D, still being too distant to form a hydrogen bond with retinal. However, during the equilibration of M_e, water D moved toward the Schiff base; the latter rotated to the cytoplasmic direction to finally establish a hydrogen-bond with water D. This move lead to a breaking of the hydrogen bond between the Schiff base and water F, as shown in Fig. 8. The hydroxyl group of water F then hydrogen bonded with water D. Thus, the waters in the cytoplasmic channel and in the counterion region were connected with each other. At this stage water C hydrogen-bonded with the oxygen of the Thr-46 hydroxyl and with the carbonyl of Phe-219. Water A disconnected from the carbonyl of Phe-219 and moved toward the Schiff base together with water D.

In M_f, water D formed an even stronger hydrogen bond with the Schiff base, such that water F was driven away from the Schiff base, and induced a further rotation of the Schiff base directly toward Asp-96. The conformation at the extracellular channel did not change significantly from M_b to M_f.

The M_g state

Annealing of M_f did not lead to significantly new conformations. Because enough space exists in the cytoplasmic channel for another water molecule, we moved water E from the far extracellular site to the place between the hydroxyl of Asp-96 and water C in an attempt to build a continuous hydrogen bond network between Asp-96 and

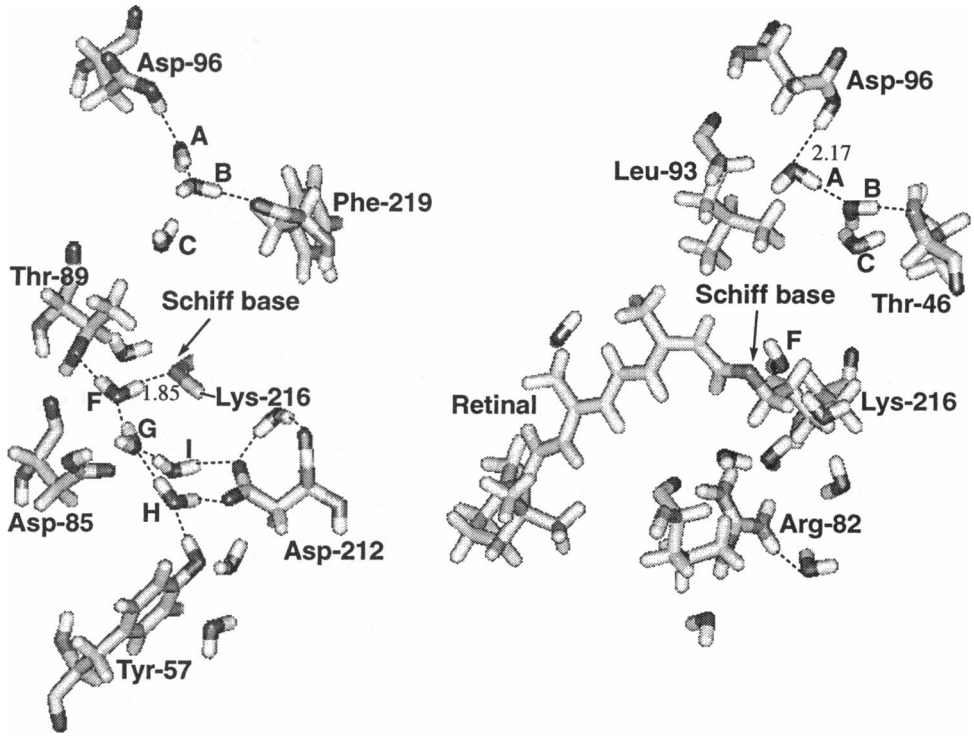

FIGURE 8 Structure of M_a in the vicinity of the retinal Schiff base, seen from two different directions. Dashed lines between atoms represent possible hydrogen bonds.

retinal. This placement resulted in structure M_g, which formed the desired hydrogen bond network between Asp-96, Thr-46, Phe-219, Lys-216 and the Schiff base, as shown in Fig. 11.

In the counterion region the hydrogen bonds between waters E, F, G, I, and H assumed an optimal geometry such that the arrangement of waters and residues around the Schiff base became more compact. An analysis of simulations also revealed that the water molecules in M_g are less mobile than in the previous stages of the M_{412} intermediate.

Recent FTIR measurements revealed that Tyr-185 undergoes a significant structural change during the $bR_{568} \rightarrow N_{520}$ transition (Ludlam et al., 1995). Our simulations show that the geometry of M_g is close to that of N_{520} formed by Asp-96 $\rightarrow$ retinal protonation around Tyr-185. The conformation of Tyr-185 in M_g, and consequently in N_{520}, is similar to that of M_a,

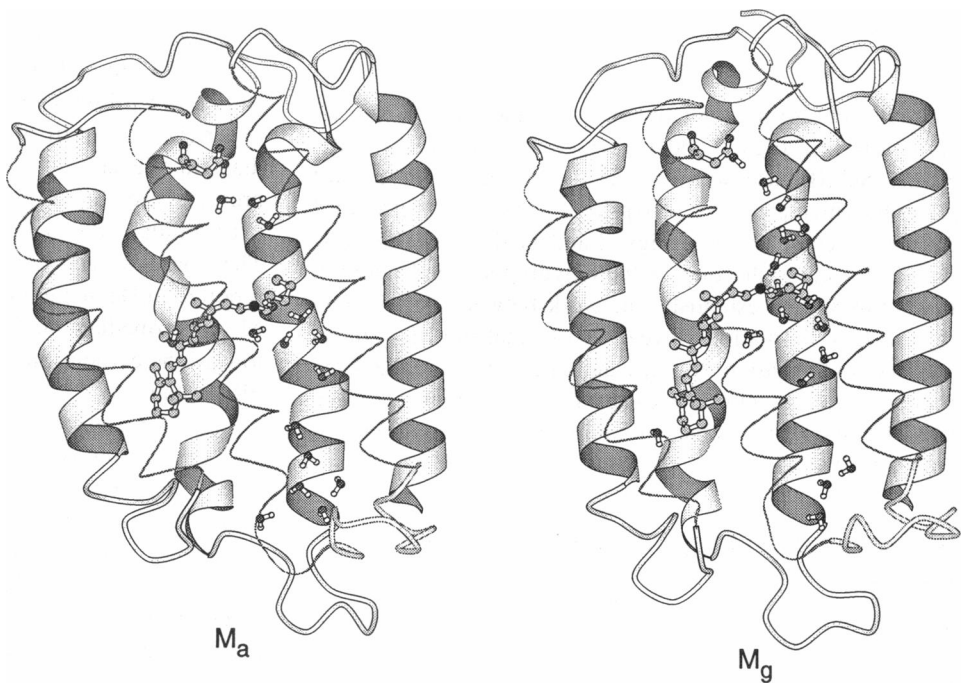

FIGURE 9 Comparison of the overall structures of M_a and M_g. From left to right, the ribbons represent helices E, F, G, and A, and the thin lines represent helices D, C, and B.

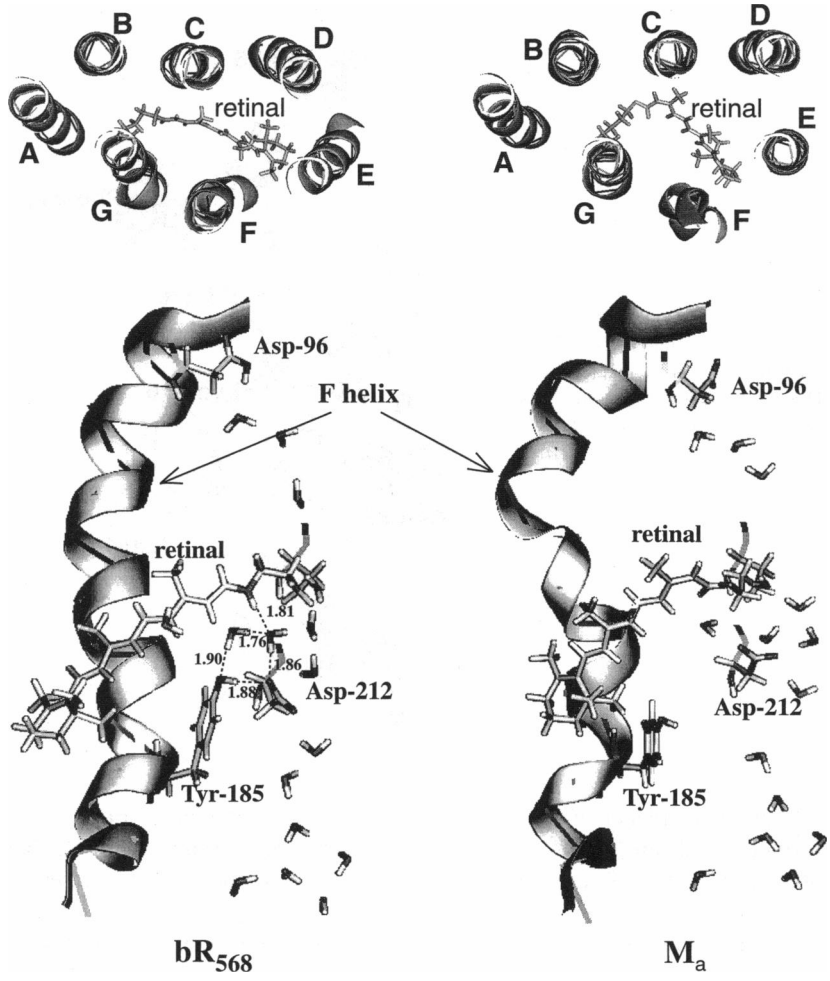

FIGURE 10 *Top*: View of the seven trans-membrane helices of bR_{568} and M_a. The tilt of helix F in M_a is seen to widen the cytoplasmic channel. *Bottom*: Conformation of helix F and its environment in bR_{568} and M_a. Dashed lines between atoms represent possible hydrogen bonds.

i.e., it moves more than 3 Å away from the Schiff base compared with its position in the structure of bR_{568}. Hence, our findings are in agreement with Ludlam et al. (1995).

Summary

Retinal's conformational dynamics at the M_{412} stage are summarized in Figs. 5 and 12, which show the twist of the retinal Schiff base nitrogen from an orientation toward water F (which connects to Asp-85) to an orientation toward Asp-96. A comparison of Figs. 8 and 11 demonstrates how water molecules disconnect their hydrogen bond network from Asp-85 and establish a network between Asp-96 and retinal. Our simulations reveal clearly that the M_{412} intermediate, in the case of the L_1 candidate of L_{550}, realizes the protein switch function necessary for proton pumping. The tilts of helix F and retinal in simulations are in agreement with observations.

Simulation of an M_{412} intermediate starting from L_2

We will now consider the evolution of bR in the case that the M_{412} stage is initiated through retinal → Asp-85 proton transfer of L_2.

The MI_a state

Proton transfer from retinal to Asp-85 in L_2 and equilibration lead to a structure denoted as MI_a. Fig. 13 presents the corresponding geometry of retinal and compares it to the geometry of retinal in bR_{568}. One notes that retinal in MI_a is shifted toward the cytoplasmic side, the methyl carbon C_{20} experiencing a shift of 4.64 Å, which is much larger than that experienced at this stage in the L_1 pathway. In the present case, the Schiff base nitrogen points toward the extracellular side, i.e., away from the proton donor Asp-96. The changes seen are at variance with the observations reported in Heyn and Otto (1992), which showed that in the M_{412} intermediate the C_{20} methyl group shifts by only 1.7 Å toward the cytoplasmic side of the membrane relative to the bR_{568} state.

Fig. 14 provides 2 views of retinal, of key amino acid side groups and of key water molecules. The three water molecules (A, B, C) in the cytoplasmic channel form a hydrogen bond network involving Thr-46 and the carbonyls of Phe-219 and Lys-216. These waters do not hydrogen-bond with Asp-96, nor, because of the opposite orientation, with retinal's Schiff base. In the counterion region and in the extracellular channel, a hydrogen-bond network of waters is formed with three water molecules

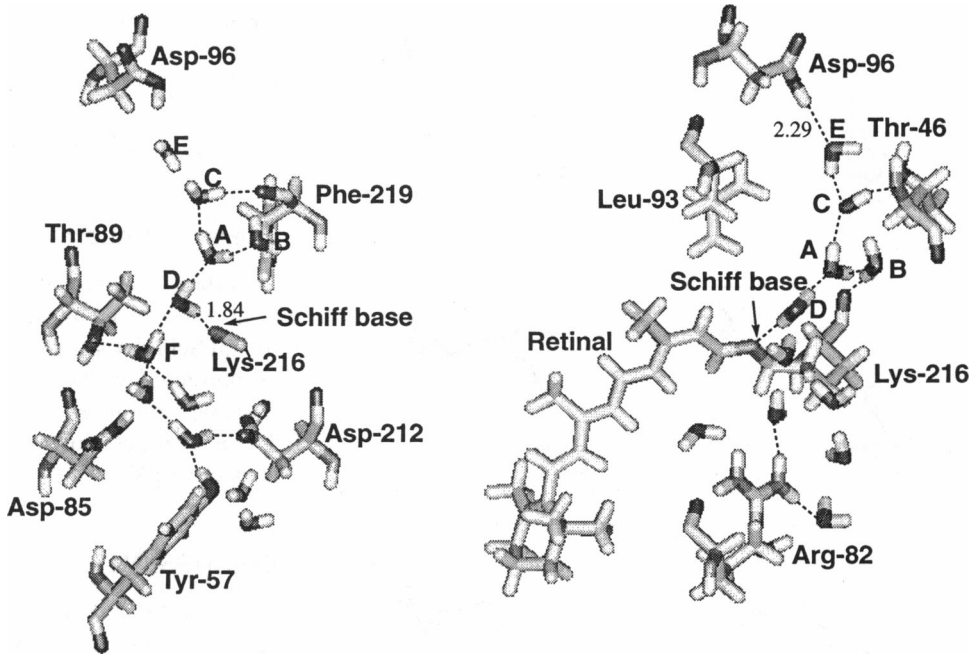

FIGURE 11 Structure of M_g in the vicinity of the retinal Schiff base, seen from two different directions. Dashed lines between atoms represent possible hydrogen bonds.

connecting residues Tyr-57, Asp-212, Thr-89, and Tyr-185. A week hydrogen bond is formed between Asp-85 and water.

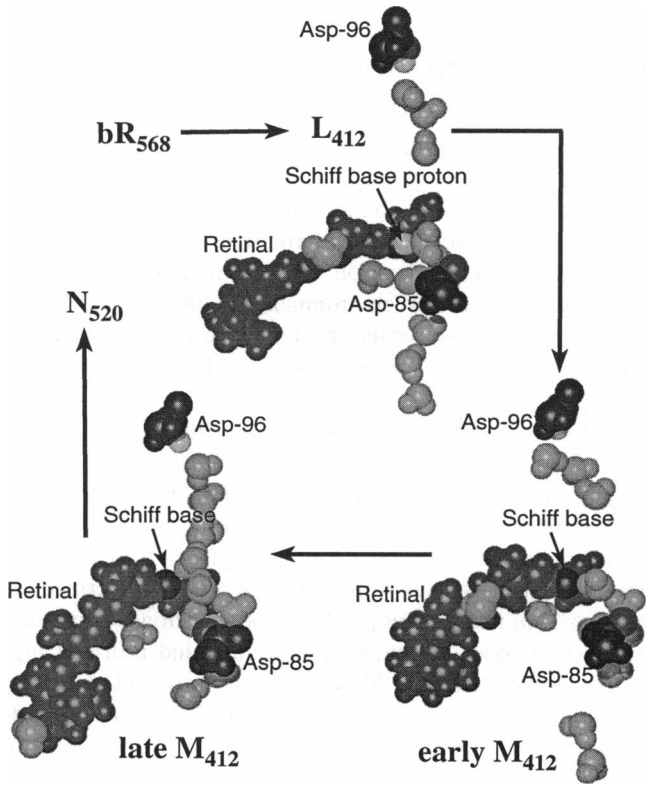

FIGURE 12 Conformational changes of retinal and water during the transition $L_{550} \rightarrow$ early $M_{412} \rightarrow$ late M_{412} of bacteriorhodopsin's photocycle. The top structure (L_{550}) corresponds to L_1. The pathway shown constitutes the most likely mechanism for proton pumping in bacteriorhodopsin according to the present investigation.

The structure MI_a exhibits a total RMSD from the structure of L_2 of 1.63 Å, which is significantly smaller than the RMSD experienced at this stage for the model of M_{412} based on the L_1 state. Fig. 15 *a* presents the overall structure of bR in MI_a. Helices F and G show only small changes compared to bR_{568}; in particular, a bent of helix F does not arise. Helices D and E exhibit larger RMSD than others.

From MI_b *to* MI_a

In MI_b, the structure of the Schiff base and the configuration of the cytoplasmic channel is almost the same as in MI_a, except that water B and Asp-96 approach each other to form a strong hydrogen bond. After the annealing of MI_b, the Schiff base still pointed down. Only during the equilibration stage after the annealing did the Schiff base gradually turn toward Asp-96 through isomerization around the 14–15 bond of retinal. At the MI_c stage, the Schiff base pointed toward Asp-96 (see Fig. 13), but did not engage in a hydrogen bond with the waters in the cytoplasmic channel. Further annealing did not lead to formation of a hydrogen bond network to connect the retinal Schiff base to Asp-96. We conclude from this that at least one more water molecule needs to be added to the cytoplasmic channel to build the needed connection between retinal and Asp-96. Accordingly, we placed a water molecule between the retinal Schiff base and its closest water to form MI_a. The overall structure of the protein did not change as a result. Water B and Asp-96 separated to assume a distance of 2.66 Å between the carboxyl hydrogen of Asp-96 and the oxygen of water B.

The MI_e *state*

After another round of simulated annealing we reached MI_e, which is represented in Fig. 16. At this stage, one can

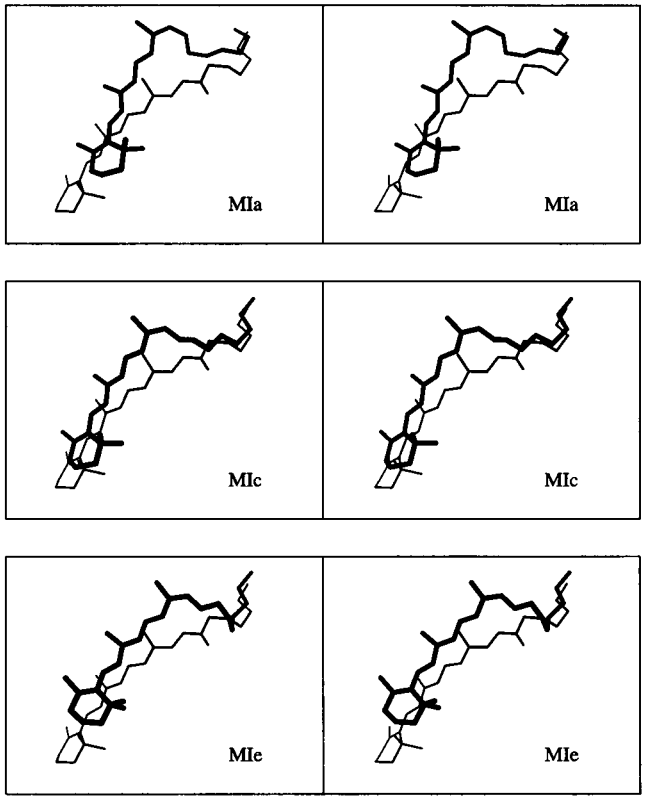

FIGURE 13 Stereoviews of retinal of MI_a, MI_c, and MI_e (*bold*) superimposed on retinal in bR_{568} (*thin*). There is no center for mass movement or overall rotation of the whole bR from bR_{568} to MI_a, MI_c, or MI_e.

discern a hydrogen bond network formed between the hydroxyl of Asp-96 and the Schiff base through four waters. We also observed a rearrangement of waters on the extracellular site of bR, as also shown in Fig. 16. It is interesting to note that an uninterrupted hydrogen bond network stretches from Asp-96 to Tyr-57 connecting the cytoplasmic and extracellular channels, in the same way as M_g.

The MI_e conformation, which is similar to that of MI_a, is close to N_{520} formed through Asp-96 → retinal proton transfer in MI_e. Tyr-185 in MI_e has much less movement relative to bR_{568} than in M_a. Hence the observation that Tyr-185 undergoes a significant structural change during the bR_{568} → N_{520} transition (Ludlam et al., 1995) is not reproduced in the simulations based on the L_2 structure for the L_{550} intermediate.

Summary

The most crucial change implied in the L_2 pathway is the 13,14-*dicis* → 13-*cis* transformation which involves a twist of the retinal Schiff base nitrogen from an orientation pointing toward Asp-85 to an orientation pointing toward Asp-96. The retinal geometrical transformations during the MI_a to MI_e sequence reflecting this twist are summarized in Fig. 13. Together with Figures 14 and 16, which present the formation of a hydrogen bond network between Asp-96 and retinal, the simulations indicate that the sequence MI_a to MI_e can also serve as a proton switch of bR. However, the MI_a to MI_e sequence does not involve a tilt of helix F (cf. Fig. 9 for the M_a state) and implies a tilt of retinal that is at variance with observations.

Interaction energies

Important information on the role of the M_{412} intermediate is also conveyed by the interaction energies between the retinal Schiff base or key amino acid side groups and water, as presented in Table 1, as well as by the energies for possible proton transfer transitions presented in Table 2. These energies do not provide quantitative measures of respective pK_a values.

DISCUSSION

Our molecular dynamics simulations allow us to discuss several key aspects of the M_{412} intermediate of bR, namely, the interactions that induce the L_{550} → M_{412} transition, the role of helix F during the M_{412} intermediate, the role of the M_{412} state as a proton switch, the forces driving the decay of the M_{412} state toward the N_{520} state, and the heterogeneity of the M_{412} intermediate. We also briefly comment on the simulated annealing method used in our simulations.

Driving forces for the L_{550} → M_{412} transition

The L_{550} → M_{412} transition involves the transfer of the retinal Schiff base proton to Asp-85. A key question regarding this transition is which interactions stabilize the protonation of Asp-85. As pointed out by Hwang and Warshel (1988), an ion pair's microenvironment plays the essential role in the ion's stabilization. Our simulations indicate that major factors of this environment in bR are the bound waters (in this case, waters bridging the protonated Schiff base and negative charges in its vicinity), and their geometry.

In fact, our simulations show that in the L_{550} intermediate, the water molecules that bridge the Schiff base and Asp-85 do not fit as tightly as in bR_{568} (Humphrey et al., 1995). This is clearly evident from the entries of Table 1, which indicate that the interaction energies of water with the retinal Schiff base and with Asp-85 in the L_{550} intermediate are less than those in bR_{568}. These observations support the suggestion based on model compounds and artificial pigments studies (Gat and Sheves, 1993; Rousso et al., 1995) that a major factor that controls the pK_a of the ion pair in bR binding site involves specific geometrical arrangements of the donor and acceptor groups and particularly the bound waters between them that allow effective stabilization of the ion pair. Observations of bR mutants also revealed that the arrangement of bound water exerts a large degree of control over the proton transfer process in the L_{550} → M_{412} transition. Neither in the case of an Asp212Asn mutation (Stern

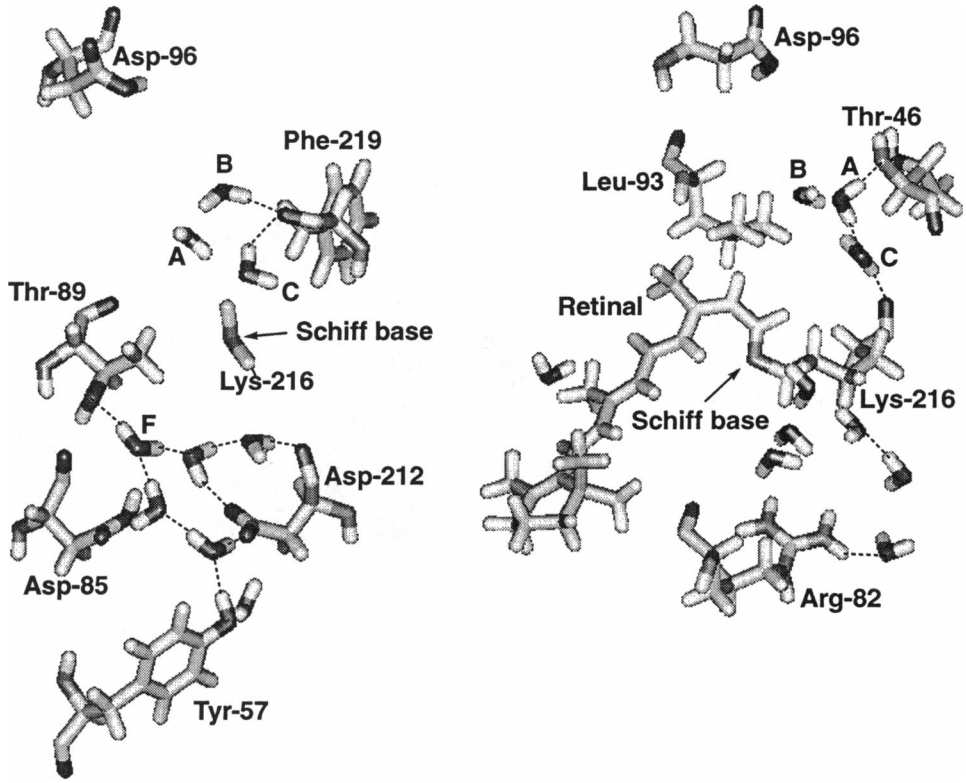

FIGURE 14 Structure of MI_a in the vicinity of the Schiff base, seen from two different directions. Dashed lines between atoms represent possible hydrogen bonds.

and Khorana, 1989; Otto et al., 1990; Rothschild et al., 1990) nor in the case of a Tyr57Asn mutation (Soppa et al., 1989) does the M_{412} intermediate form at pH = 7. Our simulations show that the mentioned residues play an important role in the hydrogen bond network. We suggest that mutation of Asp-212 or Tyr-57 alters the water environment around the Schiff base during the photocycle and thereby renders the $L_{550} \rightarrow M_{412}$ transition unfavorable. The importance of protein structural changes for the stabilization of M_{412}, i.e., for change of the pK_a value of the protonated Schiff base and a shift of the equilibrium toward the unprotonated Schiff base, was suggested previously (Koutalos et al., 1990). Our simulations suggest a specific structure for the hydrogen bond network of water between the Schiff

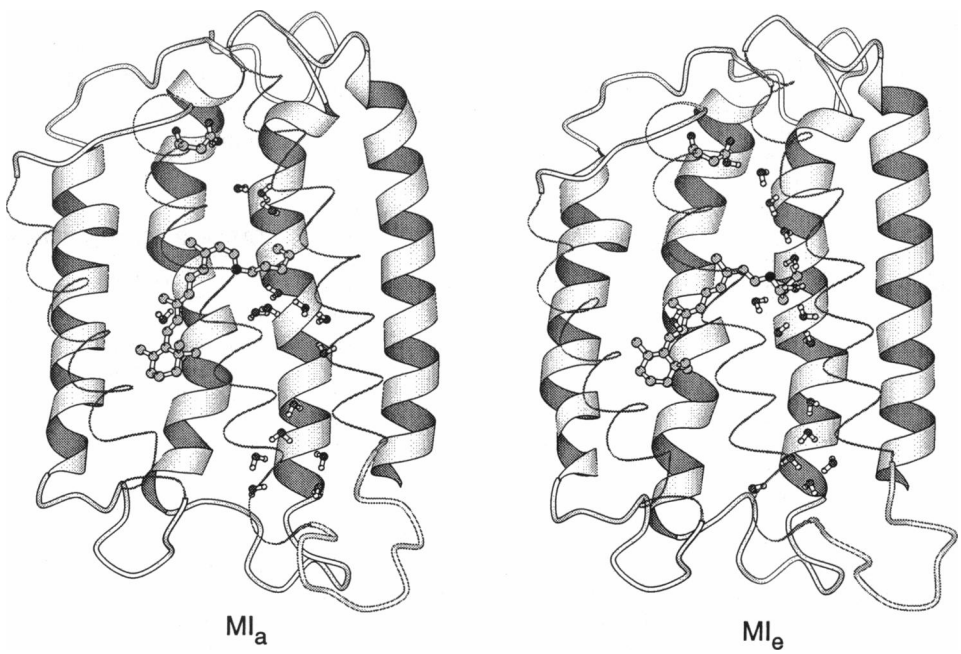

FIGURE 15 Comparison of the overall structures of MI_a and MI_c. From left to right, the ribbons represent helices E, F, G and A and the thin lines represent helices D, C, and B.

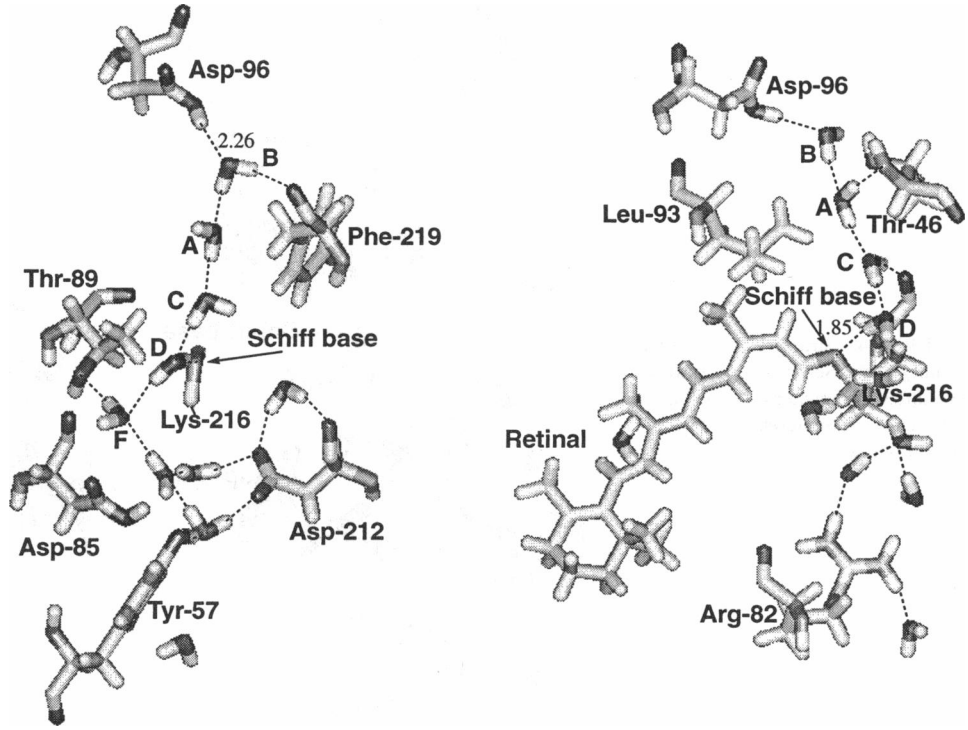

FIGURE 16 Structure of MI_e in the vicinity of the Schiff base, seen from two different perspectives. Dashed lines between atoms represent possible hydrogen bonds.

base, Asp-212, Arg-82, Thr-89, and Tyr-57, which plays an important role in stabilizing the M_{412} intermediate.

Following proton transfer to Asp-85, the interaction between Asp-85 and water is weakened significantly, as shown in the entries of Table 1 and as illustrated through the hydrogen bond network shown in Figs. 8 and 14. These results are consistent with FTIR measurements (Engelhard et al., 1985, Braiman et al., 1991) that indicate that Asp-85 is in a hydrophobic environment at the M_{412} stage.

TABLE 1 Interaction energies between key groups and water

Stage	Schiff base (N or NH)	Asp-85 (COO^- or COOH)	Asp-96 (COOH)
bR_{568}	−9.3	−22.5	−8.8
L_1	−6.6	−13.2	−7.4
M_a	−14.4	−0.8	−8.5
M_b	−14.3	−3.1	−9.7
M_c	−16.0	−2.2	−0.5
M_d	−15.8	−4.6	−1.6
M_e	−14.2	−1.8	−0.4
M_f	−10.2	−2.0	−0.3
M_g	−12.3	−3.9	−6.6
L_2	−1.8	−26.8	0.0
MI_a	1.0	−8.1	−0.3
MI_b	1.4	−1.7	−2.7
MI_c	−1.3	−12.3	−7.1
MI_d	−13.2	−11.1	−1.4
MI_e	−14.5	−5.0	−5.7

The values (in units of kcal/mol) listed in the table are the sum of electrostatic and explicit hydrogen bonding interaction energies between the particular group listed in the table and all the water molecules placed in bR. Structures used for the calculation of these energies were obtained through energy minimization of the respective equilibrated structures.

As shown in Table 2, our simulations indicate that the $L_{550} \rightarrow M_{412}$ transition is a strongly activated process if we view M_a or MI_a as a product of L_1 or L_2. The energy for an immediate proton transfer in the L_1 or the L_2 state is actually positive (52 or 60 kcal/mol respectively). The transition becomes possible only through stabilization of the resulting state by 74 kcal/mol in the subsequent 20-ps equilibration process between L_1 and M_a involving an optimal hydrogen bond network in the counterion region (the energy difference before and after the proton transfer, i.e., between L_1 and M_a is now −22 kcal/mol). In contrast, transfer of a proton in bR_{568} from the Schiff base to Asp-85 is also strongly activated (62 kcal/mol), but in the latter case subsequent equilibration does not stabilize the system as strongly as in the L_1 case (37 kcal/mol). Although the numbers of energies may not be exact because of errors in

TABLE 2 Energy difference for proton transfer reactions

Transition	Transfer (a)	Transfer and eqn (b)
bR_{568} (retinal → Asp-85)	62	37
L_1 (retinal → Asp-85)	52	−22
L_2 (retinal → Asp-85)	60	14
M_g (Asp-96 → retinal)	−30	−72
MI_e (Asp-96 → retinal)	−11	−45

Energies (in units of kcal/mol) connected with various proton transfers, i.e., the differences in the total potential energy of bR before and after the respective transitions. The energies after the transition were calculated in two ways: (a) transfer of the proton from the Schiff base to Asp-85 to form a possible M_{412} state, or transfer of the proton from Asp-96 to the Schiff base leading to a possible N_{520} state; (b) same as (a), but including a 20-ps equilibration at 300 K after the proton transfer. Energies were calculated from minimized structures.

energy calculations, the strong tendency appears to show that the conformational rearrangement during proton transfer in the L_{550} state is very important for the stabilization of the M_{412} intermediate.

Shift of retinal spectrum in M_{412}

The formation of optimal hydrogen bonds around the retinal Schiff base linkage in the initial M_{412} state can also explain why the spectrum of retinal is strongly red-shifted at this stage of the photocycle relative to the spectrum of the unprotonated Schiff base of retinal in solution, the latter absorbing at 360 nm (Gat and Sheves, 1994). It had been suggested previously that this red shift originates from an effective hydrogen bond of the Schiff base with internal water or with protein residues (Gat and Sheves, 1994). Our simulations suggest that the red shift is due to hydrogen bonding between a structured water and the Schiff base. As shown in Table 1, as well as indicated in the structures shown in Figs. 8 and 11, the Schiff base has significantly stronger interaction with water in all stages of M_{412} in the L_1 pathway and in later stages of the L_2 pathway than it has in the L_{550} intermediate or in bR_{568}.

The role of helix F

The bend of helix F is a key attribute of the M_{412} intermediate which raises the question of what interactions induce it. Unfortunately, our simulations do not give a clear answer. To understand the mechanism of the bending of helix F we have carried out simulations with modified structures.

The bend arises only after deprotonation of retinal in an L_1 conformation and does not arise after deprotonation of retinal with bR in an L_2 conformation. FTIR measurements indicate that amide bonds experience structural alterations following M_{412} formation (Braiman et al., 1987). The changes might be associated with the conformational changes of the F and G helices, characterized by the destruction of the hydrogen bonds along α-helices between amide groups and carbonyls, including changes of the hydrogen bonds of carbonyls of Lys-216 and Phe-219 on helix G. Recent studies have shown that the Lys-216 carbonyl exhibits a very low stretching frequency in the M_{412} intermediate, and it has been suggested that the carbonyl experiences a strong hydrogen bond with bound water (Takei et al., 1994). This suggestion is supported by our simulations. The conformational changes of helical backbones are also in agreement with the finding reported in Subramanian et al. (1993), except that a translational change of helix E predicted by our simulations was not observed.

In our simulations, the bend of helix F diminishes in going from M_a to M_d, and disappears altogether for M_e when the waters in the cytoplasmic channel become ordered and form a hydrogen bond network with the Schiff base. This result suggests that the bend of helix F is affected by the waters in the cytoplasmic channel. Indeed, simulations in which the three water molecules in the cytoplasmic channel were removed at the M_a stage yielded a significantly smaller bend of helix F. In the case that all 16 water molecules in the bR interior are removed at the M_a stage, no significant bend of helix F arises. This finding might explain the previously reported electron diffraction data (Glaeser et al., 1986), which did not reveal protein structural changes at the M_{412} stage of bR's photocycle for dried, glucose-embedded specimens. As discussed in Results, the waters in the cytoplasmic channel are destabilized at the M_a stage. We suggest that because of the proton transfer from the protonated Schiff base to Asp-85, the dipole moment of the Schiff base and its counterion region changes, which affects the water in the cytoplasmic channel and ultimately helix F.

In order to investigate further the causes for the bending of helix F following retinal $\rightarrow$ Asp-85 proton transfer in L_1, we also carried out the simulations for a protein structure characterized by removal of the retinal chromophore from L_1 structure. A proton was transferred from Lys-216 amino group to Asp-85. In addition we tested retinal $\rightarrow$ Asp-85 proton transfer in bR_{568}. Neither of the above simulations induced significant bends of helix F after 20-ps dynamics at 300 K. The findings show that retinal contributes to the bend of the helix. Apparently, the restructuring of the water and amino acid side groups in the counterion region following proton transfer, exhibiting an energy of stabilization of 74 kcal/mol, also contributes to the bending of the helix.

The M_{412} state as a proton switch

The M_{412} state plays a key role as a proton switch in the pump cycle of bR, M_{412} being formed by transfer of a proton that feeds to the extracellular space and M_{412} decaying through transfer of a proton fed from the cytoplasmic side. Our simulations suggest specific roles of retinal, of the protein, and of the internal waters in this respect. As pointed out above, experimental evidence favors the simulated M_{412} intermediate that results from the L_1 structure for L_{556} suggested in Humphrey et al. (1995) rather than an M_{412} derived from the L_2 structure. Fig. 12 summarizes the mechanism of the light-driven proton pump that emerges from this finding. The role of the phototransformation is to prepare a stereochemically specific intermediate, namely, the L_1 structure, in which the plane of the Schiff base nitrogen and its two neighboring carbon atoms points parallel to the membrane plane toward a water molecule that provides a direct hydrogen bond contact to the primary proton acceptor Asp-85. Immediately after the proton transfer, retinal remains in the stated geometry, but at the late stage of M_{412} the retinal nitrogen turns toward Asp-96, i.e., toward the proton donor. The motion, triggered by cytoplasmic water approaching the Schiff base linkage, involves only a small redirection of retinal, which is in agreement with linear dichroism data (Heyn and Otto, 1992), but requires a significant motion of the chain of Lys-216 (Fig. 7) as shown in Gat et al. (1992).

Our simulations suggest that in the early stage of M_{412} the dipole moment of the complex of water, retinal, and amino acid side groups in the counterion region is changed, which influences the arrangement of water in the cytoplasmic channel and triggers a conformational change of the protein on the cytoplasmic side, in particular, helices F and G. An opening of the cytoplasmic channel allows more water to enter the channel, to approach the Schiff base linkage region, and to form a complete hydrogen bridge network between Asp-96 and the reoriented retinal Schiff base nitrogen. Comparing the structure of M_a and M_g in Figs. 8 and 11, one can see that water molecules around the Schiff base in M_g engage in more extended hydrogen bonds than in the M_a stage. Such rearrangement of water implies a significant ordering of water and, hence, an entropy reduction as is, in fact, observed in Ort and Parson (1979) and Váró and Lanyi (1991a). The retinal, the protein, and the water in the late stage of M_{412} are perfectly set up for the Asp-96 → retinal proton transfer connected with the decay of M_{412} and the formation of the N_{520} intermediate.

Decay of M_{412}

Experimental evidence indicated that the decay of M_{412} is significantly slowed down under low humidity conditions (Korenstein and Hess, 1977, Lechner et al., 1994) or by using osmotically active solute (Cao et al., 1991), which shows that water plays an important role in the Schiff base protonation and in the subsequent stages associated with the decay of M_{412}. The waters in the cytoplasmic channel, which connect Asp-96 to the Schiff base, are located between helices B, C, and G. These waters make direct contact with the hydroxyl group of Thr-46 on helix B, the Lys-216 and Phe-219 carbonyls on helix G, constituting a hydrophilic environment. The mentioned groups stabilize the water chain between Asp-96 and the Schiff base through hydrogen bonds as born out by a Thr-46 to Val-46 mutation, which shows a slow M_{412} decay (Marti et al., 1991; Subramaniam et al., 1991; Brown et al., 1993, 1994). The other side of the water chain is surrounded by hydrophobic groups, i.e., Phe-42 on helix B, Leu-93 on helix C, Phe-219 on helix G, Val-49 on helix B the methyl group of Thr-89 on helix C, and the C_{20} methyl group of retinal. These groups interact unfavorably with waters and force them to develop good hydrogen bonds with each other and with the hydrophilic side of the cytoplasmic channel. As a result, the water may transfer a proton according to the Grothues mechanism (Brünger et al., 1983; Nagle and Tristram-Nagle, 1983). On the other hand, as pointed out by Warshel (1979), (1986), the hydrogen bond network between donor and receptor is not sufficient to make the proton transfer, and energetics is the final criterion to determine the possibility of proton transfer. A proton transfer chain requires a network of groups with low pK_a (Warshel, 1978). The energetics of proton transfer in bR still needs further studies.

The simulations suggest that water reorganizations in the cytoplasmic region during M_{412} is also made possible by conformational changes involving Leu-93, which allows easier access of water to the retinal's Schiff base. This suggestion is corroborated by the observation that a Leu-93 to Ala-93 mutation exhibits faster M_{412} decay than native bR (Subramaniam et al., 1991); the mutant provides more space in the channel to allow easier water access. The C_{20} methyl group of retinal blocks Leu-93 from moving toward retinal and thereby maintains the structure of the water channel. It is predicted by the simulations that without the C_{20} methyl group, Leu-93 will move toward the Schiff base and will block water from binding to the nitrogen of the Schiff base, such that a continuous proton transfer chain between Asp-96 and retinal is not established.

Heterogeneity of M_{412}

The simulations indicate that M_{412} is a very heterogeneous intermediate and should be considered a sequence of states, i.e., a process, rather than a distinct state. Experiments showed that there are at least two components to the M_{412} intermediate (Váró et al., 1992; Druckman et al., 1992; Takei and Lewis, 1993), a third component being suggested as well (Sasaki et al., 1992). A low temperature study demonstrated recently that M_{412} consists of five substates (Friedman et al., 1994). The many M_{412} substates characterized in our simulations fall into two classes, i.e., those before the turn of the retinal nitrogen from water F toward Asp-96 (Fig. 8) and those after the turn (Fig 11).

The many metastable substates of M_{412} captured in our simulations do not necessarily have to occur in the same sequence as in our simulation; the actual M_{412} state, e.g., as observed spectroscopically, may constitute an ensemble of all these substates in quasi-equilibrium such that these M_{412} substates may not be easily distinguished through their absorption spectra. The heterogeneity of the M_{412} intermediate can also be understood through the suggestion in Austin et al. (1975) and Frauenfelder et al. (1979), i.e., that proteins exhibit a large number of nearly isoenergetic substates: the M_{412} intermediate of bR appears to involve two classes of substates, M_I and M_{II}, each class constituting a large number of metastable states.

Justification for simulated annealing

Finally, we would like to comment on the relationship between the actual dynamics of a protein and its description through simulated annealing. It is surprising that simulated annealing lead us to results in agreement with our observations. One possible reason is that the native bR is robust under changes of environmental factors like pressure and temperature, such that the key features of the M_{412} intermediate are still preserved in a simulated annealing description. The results suggest to employ simulated annealing to other biomolecules to bridge the long time scale that current molecular dynamics simulations cannot access.

We thank J. Lanyi, B. Roux, J. Herzfeld, W. Humphrey, I. Logunov, and F. Zhou for helpful discussions. Most simulations presented in this paper were carried out on Silicon Graphics and Hewlett-Packard workstations operated by the Resource for Concurrent Biological Computing at the University of Illinois and were funded by the National Institutes of Health (grant PHS 5 P41 RR05969–04). Some simulations were done on a Cray 2 computer operated by the National Center for Supercomputing Applications at the University of Illinois and were funded by the National Science Foundation.

REFERENCES

Aton, B., A. G. Doukas, R. H. Callender, B. Becker, and T. G. Ebrey. 1977. Resonance raman studies of the purple membrane. *Biochemistry.* 16: 2995–2999.

Austin, R. H., and L. K. W. B. Eisenstein, H. Frauenfelder, and I. C. Gunsalus. 1975. Dynamics of ligand binding to myoglobin. *Biochemistry.* 14:5355.

Bashford, D. and K. Gerwert. 1992. Electrostatic calculations of the pK values of ionizable groups in bacteriorhodopsin. *J. Mol. Biol.* 224: 473–486.

Braiman, M. S., P. L. Ahl, and K. J. Rothschild. 1987. Millisecond Fourier-transform infrared difference spectra of bacteriorhodopsin's M_{412} photoproduct. *Proc. Natl. Acad. Sci. USA.* 84:5221–5225.

Braiman, M. S., O. Bousche, and K. J. Rothschild. 1991. Protein dynamics in the bacteriorhodopsin photocycle: submillisecond Fourier transform infrared spectra of the L, M, and N photointermediates. *Proc. Natl. Acad. Sci. USA.* 88:2388–2392.

Braiman, M. S., T. Mogi, T. Marti, L. J. Stern, H. G. Khorana, and K. J. Rothschild. 1988. Vibrational spectroscopy of bacteriorhodopsin mutants: light-driven proton transport involves protonation changes of aspartic acid residues 85, 96, and 212. *Biochemistry.* 27:8516–8520.

Brooks, B. R., R. E. Bruccoleri, B. D. Olafson, D. J. States, S. Swaminathan, and M. Karplus. 1983. CHARMm: a program for macromolecular energy, minimization, and dynamics calculations. *J. Comp. Chem.* 4:187–217.

Brown, L. S., Y. Yamazaki, A. Maeda, L. Sun, R. Needleman, and J. K. Lanyi. 1994. The proton transfers in the cytoplasmic domain of bacteriorhodopsin are facilitated by a cluster of interacting residues. *J. Mol. Biol.* 239:401–414.

Brown, L. S., L. Zimanyi, R. Needleman, M. Ottolenghi, and J. K. Lanyi. 1993. Photoreaction of the N-intermediate of bacteriorhodopsin, and its relationship to the decay kinetics of the M-intermediate. *Biochemistry.* 32:7679–7685.

Brünger, A. 1991. Simulated annealing in crystallography. *Ann. Rev. Phys. Chem.* 42:197–223.

Brünger, A. T. 1992. X-PLOR, Version 3.1, A System for X-ray Crystallography and NMR. The Howard Hughes Medical Institute and Department of Molecular Biophysics and Biochemistry, Yale University, New Haven, CT.

Brünger, A. T., A. Krukowski, and J. Erickson. 1990. Slow-cooling protocols for crystallographic refinement by simulated annealing. *Acta Cryst.* A46:585–593.

Brünger, A., Z. Schulten, and K. Schulten. 1983. A network thermodynamic investigation of stationary and non-stationary proton transport through proteins Z. *Phys. Chem.* NF136:1–63.

Cao, Y., G. Váró, M. Chang, B. Ni, R. Needleman, and J. K. Lanyi. 1991. Water is required for proton transfer from aspartate-96 to the bacteriorhodopsin Schiff base. *Biochemistry.* 74:10972–10979.

Dencher, N. A., J. Heberle, G. Büldt, H.-D. Höltje, and M. Höltje. 1992. Light- and dark-adapted bacteriorhodopsin, a time-resolved neutron diffraction study. *In* Membrane Proteins: Structure, Interactions and Models. A. Pullman, J. J. & B. Pullman, editor. Kluwer Academic Publishers, the Netherlands. 69–84.

Doig, S. J., P. J. Reid, and R. A. Mathies. 1991. Picosecond time-resolved resonance Raman spectroscopy of bacteriorhodopsin's J, K, and KL intermediates. *J. Phys. Chem.* 95:6372–6379.

Druckman, L. S., N. Friedman, J. K. Lanyi, R. Needleman, M. Ottolenghi, and M. Sheves. 1992. The back photoreaction of the M-intermediate in the photocycle of bacteriorhodopsin-mechanism and evidence for 2 M-species. *Photochem. Photobiol.* 56:1041–1047.

Engelhard, M., K. Gerwerk, B. Hess, W. Kreutz, and F. Siebert. 1985. Light-driven protonation changes of internal aspartic acid of bacteriorhodopsin: an investigation by static and time-resolved infrared difference spectroscopy using [4–13C] aspartic acid labeled purple membrane. *Biochemistry.* 24:400–407.

Englehard, M., B. Hess, G. Metz, W. Kreutz, F. Siebert, J. Soppa, and D. Oesterhelt. 1990. High resolution ^{13}C-solid state NMR of bacteriorhodopsin: assignment of specific aspartic acids and structural implications of single site mutations. *Eur. Biophys. J.* 18:17–24.

Fodor, S. P. A., J. B. Ames, R. Gebhard, E. M. M. van den Berg, W. Stoeckenius, J. Lugtenburg, and R. A. Mathies. 1988. Chromophore structure in bacteriorhodopsin's N intermediate: implications for the proton-pumping mechanism. *Biochemistry.* 27:7097–7101.

Frauenfelder, H., G. A. Petsko, and D. Tsernoglou. 1979. Temperature-dependent x-ray diffraction as a probe of protein structural dynamics. *Nature.* 280:558.

Friedman, N., Y. Gat, M. Sheves, and M. Ottolenghi. 1994. On the heterogeneity of the M population in the photocycle of bacteriorhodopsin. *Biochemistry.* 33:14758–14767.

Gat, Y., M. Grossjean, I. Pinevsky, H. Takei, Z. Rothman, H. Sigrist, A. Lewis, and M. Sheves. 1992. Participation of bacteriorhodopsin active-site lysine backbone in vibrations associated with retinal photochemistry. *Proc. Natl. Acad. Sci. USA.* 89:2434–2438.

Gat, Y., and M. Sheves. 1993. A mechanism for controlling the pK_a of the retinal protonated Schiff base in retinal proteins. A study with model compounds. *J. Am. Chem. Soc.* 115:3772–3773.

Gat, Y., and M. Sheves. 1994. The origin of the red-shifted absorption maximum of the M(412) intermediate in the bacteriorhodopsin photocycle. *Photochem. Photobiol.* 59:371–378.

Gerwert, K. 1992. Molecular reaxtion mechanism of photosynthetic proteins as determined by FTIR-spectroscopy. *Biochim. Biophys. Acta.* 1101:147–153.

Gerwert, K., B. Hess, J. Soppa, and D. Oesterhelt. 1989. Role of Asp-96 in proton translocation by bacteriorhodopsin. *Proc. Natl. Acad. Sci. USA.* 86:4943–4947.

Gerwert, K., and F. Siebert. 1986. Evidence for light-induced 13-*cis* 14-s-*cis* isomerization in bacteriorhodopsin obtained by Fourier transform IR difference spectrometry. *EMBO J.* 4:805–812.

Glaeser, R., J. Baldwin, T. A. Ceska, and R. Henderson. 1986. Electron diffraction analysis of the M_{412} intermediate of bacteriorhodopsin. *Biophys. J.* 50:913–920.

Hauss, T., G. Buldt, M. P. Heyn, and N. A. Dencher. 1994. Light-induced isomerization causes an increase in the chromophore tilt in the M intermediate of bacteriorhodopsin—a neutron diffraction study. *Proc. Natl. Acad. Sci. USA.* 91:11854–11858.

Henderson, R., J. M. Baldwin, T. A. Ceska, F. Zemlin, E. Beckmann, and K. H. Downing. 1990. Model for the structure of bacteriorhodopsin based on high-resolution electron cryo-microscopy. *J. Mol. Biol.* 213: 899–929.

Heyn, M. P., and H. Otto. 1992. Photoselection and transient linear dichroism with oriented immobilized purple membranes: evidence for motion of the C(20)-methyl group of the chromophore towards the cytoplasmic side of the membrane. *Photochem. Photobiol.* 56: 1105–1112.

Humphrey, W., I. Logunov, K. Schulten, and M. Sheves. 1994. Molecular dynamics study of bacteriorhodopsin and artificial pigments. *Biochemistry.* 33:3668–3678.

Humphrey, W., D. Xu, K. Schulten, and M. Sheves. 1995. Molecular dynamics study of the early intermediates in the bacteriorhodopsin photocycle. *J. Phys. Chem.* In press.

Hwang, J.-K., and A. Warshel. 1988. Why ion pair reversal by protein engineering is unlikely to succeed. *Nature.* 334:270–272.

Jorgensen, W. L., J. Chandrasekhar, J. D. Madura, R. W. Impey, and M. L. Klein. 1983. Comparison of simple potential functions for simulating liquid water. *J. Chem. Phys.* 79:926–935.

Korenstein, R., and B. Hess. 1977. Hydration effects on *cis-trans* isomerization of bacteriorhodopsin. *FEBS Lett.* 82:7–11.

Koutalos, Y., T. G. Ebrey, H. R. Gilson, and B. Honig. 1990. Octopus photoreceptor membranes. Surface charge density and pK of the schiff base of the pigments. *Biophys. J.* 58:493–501.

Kraulis, P. 1991. MOLSCRIPT—a program to produce both detailed and schematic plots of protein structures. *J. Appl. Cryst.* 24:946–950.

Lechner, R. E., N. A. Dencher, J. Fitter, and T. Dippel. 1994. 2-dimensional proton diffusion on purple membrane. *Solid State Ionics.* 40: 296–304.

Lozier, R. H., R. A. Bogomolni, and W. Stoeckenius. 1975. Bacteriorhodopsin: a light-driven proton pump in halobacterium halobium. *Biophys. J.* 15:955–962.

Ludlam, C. F. C., S. Sonar, C. P. Lee, M. Coleman, J. Herzfeld, U. L. Rajbhandary, and K. J. Rothschild. 1995. Site-directed isotope labeling and ATR-FTIR difference spectroscopy of bacteriorhodopsin—the peptide carbonyl group of Tyr 185 is structurally active during the bR → N transition. *Biochemistry.* 34:2–6.

Marti, T., H. Otto, and M. Tatsushi. 1991. Bacteriorhodopsin mutants containing single substitutions of serine or threonine residues are all active in proton translocation. *J. Biol. Chem.* 266:6919–6927.

Metz, G., F. Siebert, and M. Engelhard. 1992. Asp85 is the only internal aspartic acid that gets protonated in the M intermediate and the purple-to-blue transition of bacteriorhodopsin. A solid-state 13C CP-MAS NMR investigation. *FEBS Lett.* 303:237–241.

Mogi, T., L. J. Stern, B. H. Chao, and H. G. Khorana. 1989. Structure-function studies on bacteriorhodopsin. 8. Substitution of the membrane-embedded Proline-50, Proline-91, and Proline-186—the effects are determined by the substituting amino-acids. *J. Biol. Chem.* 264: 14192–14196.

Nagle, J. F., and S. Tristram-Nagle. 1983. Hydrogen bonded chain mechanism for proton conduction and proton pumping. *J. Membr. Biol.* 74:1–14.

Orlandi, G., and K. Schulten. 1979. Coupling of stereochemistry and proton donor-acceptor properties of a Schiff base: a model of a light-driven proton pump. *Chem. Phys. Lett.* 64:370–374.

Ort, D. R., and W. W. Parson. 1979. Enthalpy changes during the photochemical cycle of bacteriorhodopsin. *Biophys. J.* 25:355–364.

Otto, H., T. Marti, M. Holz, T. Mogi, L. J. Stern, F. Engel, H. G. Khorana, and M. P. Heyn. 1990. Substitution of amino acids Asp-85, Asp-212, and Arg-82 in bacteriorhodopsin affects the proton release phase of the pump and the pK of the Schiff base. *Proc. Natl. Acad. Sci. USA.* 87:1018–1022.

Papadopoulos, G., N. Dencher, G. Zaccai, and G. Büldt. 1990. Water molecules and exchangeable hydrogen ions at the active centre of bacteriorhodopsin localized by neutron diffraction. *J. Mol. Biol.* 214: 15–19.

Pettei, M. J., A. P. Yudd, K. Nakanishi, R. Henselman, and W. Stoeckenius. 1977. Identification of retinal isomers isolated from bacteriorhodopsin. *Biochemistry.* 16:1955–1959.

Rothschild, K. J., M. S. Brainman, and Y. W. He. 1990. Vibrational spectroscopy of bacteriorhodopsin mutants. Evidence for the interaction of aspartic acid 212 with tyrosine 185 and possible role in the proton pump mechanism. *J. Biol. Chem.* 265:16985–16991.

Rousso, I., I. Brodsky, A. Lewis, and M. Sheves. 1995. The role of water in retinal complexation to bacteriorhodopsin. *J. Biol. Chem.* 270: 13860–13868.

Sasaki, J., Y. Shichida, J. K. Lanyi, and A. Maeda. 1992. Protein changes associated with reprotonation of the schiff base in the photocycle of ASP(96) → ASN bacteriorhodopsin—the M(N) intermediate with unprotonated schiff base but N-like protein structure. *J. Biol. Chem.* 267:20782–20786.

Scharnagl, C., J. Hettenkofer, and S. F. Fischer. 1994. Proton release pathway in bacteriorhodopsin: molecular dynamics and electrostatic calculations. *Int. J. Quantum Chem: Bio. Symp.* 21:33–56.

Schulten, K. 1978. An isomerization model for the photocycle of bacteriorhodopsin. *In* Energetics and Structure of Halophilic Organisms. S. R. Caplan, and M. Ginzburg, editor. Elsevier. 331–334.

Schulten, K., Z. Schulten, and P. Tavan. 1984. An isomerization model for the pump cycle of bacteriorhodopsin. *In* Information and Energy Transduction in Biological Membranes. L. Bolis, E. J. M. Helmreich, and H. Passow, editors. Allan R. Liss, Inc., New York. 113–131.

Schulten, K., and P. Tavan. 1978. A mechanism for the light-driven proton pump of *Halobacterium halobium. Nature.* 272:85–86.

Soppa, J., J. Otomo, L. Straub, J. Tittor, S. Messen, and D. Oesterhelt. 1989. Bacteriorhodopsin mutants of *Halobacterium sp.* GRB. characterization of mutants. *J. Biol. Chem.* 264:13049–13056.

Stern, L. J., and H. G. Khorana. 1989. Structure-function studies on bacteriorhodopsin. Individual substitutions of arginine residues by glutamine affect chromophore formation, photocycle, and proton translocation. *J. Biol. Chem.* 264:14202–14208.

Subramaniam, S., S. J. T. M. Rösselet, K. J. Rothschild, and H. G. Khorana. 1991. The reaction of hydroxylamine with bacteriorhodopsin studied with mutants that have altered photocycles: selective reactivity of different photointermediates. *Proc. Natl. Acad. Sci. USA.* 88: 2583–2587.

Subramanian, S., M. Gerstein, D. Oesterhelt, and R. Henderson. 1993. Electron diffraction analysis of structural changes in the photocycle of bacteriorhodopsin. *EMBO J.* 12:1–8.

Takei, H., Y. Gat, Z. Rothman, A. Lewis, and M. Sheves. 1994. Active site lysine backbone undergoes conformational changes in the bacteriorhodopsin photocycle. *J. Biol. Chem.* 269:7387–7389.

Takei, H., and A. Lewis. 1993. Biphasic-M decay of high pH dehydrated purple membrane studied with Fourier transform infrared spectroscopy—a model accounting for functional differences between different M-forms. *Photochem. Photobiol.* 57:707–713.

van Laarhoven, P. J. M., and E. H. L. Aarts. 1987. *Simulated Annealing: Theory and Application.* D. Riedel, Dordrecht, the Netherlands.

Váró, G., A. Duschl, and J. K. Lanyi. 1990. Interconversions of the M, N, and O intermediates in the bacteriorhodopsin photocycle. *Biochemistry.* 29:3798–3804.

Váró, G., and J. K. Lanyi. 1990. Protonation and deprotonation of the M-intermediate, N-intermediate, and O-intermediate during the bacteriorhodopsin photocycle. *Biochemistry.* 29:6858–6865.

Váró, G., and J. K. Lanyi. 1991a. Thermodynamics and energy coupling in the bacteriorhodopsin photocycle. *Biochemistry.* 30:5016–5022.

Váró, G., and J. K. Lanyi. 1991b. Kinetic and spectroscopic evidence for an irreversible step between deprotonation and reprotonation of the Schiff-base in the bacteriorhodopsin photocycle. *Biochemistry.* 30: 5008–5015.

Váró, G., L. Zimanyi, M. Chang, B. F. Ni, R. Needleman, and J. K. Lanyi. 1992. A residue substitution near the β-ionone ring of the retinal affects the M substates of bacteriorhodopsin. *Biophys. J.* 61:820–826.

Warshel, A. 1978. Energetics of enzyme catalysis. *Proc. Natl. Acad. Sci. USA.* 75:5250–5254.

Warshel, A. 1979. Conversion of light energy to electrostatic energy in the proton pump of *Halobacterium halobium. Photochem. Photobiol.* 30: 285–290.

Warshel, A. 1986. Correlation between the structure and efficiency of light-induced proton pumps. *Methods in Enzymology.* 127:578–587.

Warshel, A., Z. T. Chu, and J.-K. Hwang. 1991. The dynamics of the primary event in rhodopsins revisited. *Chem. Phys.* 158:303–314.

Zhou, F., A. Windemuth, and K. Schulten. 1993. Molecular dynamics study of the proton pump cycle of bacteriorhodopsin. *Biochemistry.* 32:2291–2306.